

Counting metastable states in a kinetically constrained model using a patch repetition analysis

Robert L. Jack

Department of Physics, University of Bath, Bath, BA2 7AY, United Kingdom

We analyse metastable states in the East model, using a recently-proposed patch-repetition analysis based on time-averaged density profiles. The results reveal a hierarchy of states of varying lifetimes, consistent with previous studies in which the metastable states were identified and used to explain the glassy dynamics of the model. We establish a mapping between these states and configurations of systems of hard rods, which allows us to analyse both typical and atypical metastable states. We discuss connections between the complexity of metastable states and large-deviation functions of dynamical quantities, both in the context of the East model and more generally in glassy systems.

PACS numbers: 64.70.Q-, 05.40-a

I. INTRODUCTION

As supercooled liquids approach their glass transitions, their viscosities (and relaxation times) increase rapidly [1, 2]. Despite a very considerable body of theoretical work, there remains no consensus as to how this observation should best be explained. In some theoretical pictures, relaxation takes place via “excitations” [3, 4] (or “soft spots” [5]) that become increasingly rare at low temperatures, slowing down the dynamics. Alternatively, one may imagine that the system evolves on a rough potential energy surface, and tends to become trapped in deep minima as the temperature is lowered [6, 7]. Or perhaps, the diversity (entropy) of disordered states decreases so strongly at low temperatures that transitions between distinct states require large-scale rearrangements that are necessarily very slow [8, 9].

In order to refine these qualitative pictures, theoretical developments are complemented by computer simulations of glassy fluids. However, the practical task of identifying objects like “excitations” or “free energy minima” in simulation is a difficult one (see however [5, 10]). A particular case in point is the idea of *metastable states*. It is very natural to describe glassy dynamics in terms of rare transitions between such states, which are also well-defined in some classes of mean-field model [11, 12]. In computer simulation, identifying distinct metastable states is possible in small systems [7], but the generalisation to extended (large) systems is more difficult (see also [13]). This is an important obstacle when attempting to test theoretical pictures based on mean-field models.

Recently, Kurchan and Levine [14] proposed a *patch-repetition analysis* whereby metastable states may be identified and characterised, using computer simulations of large systems. The method has two main components: a time-averaging procedure that associates metastable states of lifetime τ with well-defined density profiles; and a counting procedure based on finite ‘patches’ of the large system. This work provides a method (or thought-experiment) by which metastable states may be defined in finite-dimensional systems. Recent numerical stud-

ies based on this method [15, 16] have focussed on the counting procedure, showing that this can indeed yield an entropy associated with the number of states in the system.

Here, we apply the patch-repetition analysis to the East model [17, 18]. This is a kinetically constrained model [19, 20] whose thermodynamic properties (and potential energy landscape) are trivial, but whose dynamics are nevertheless complex, and have striking similarities with molecular glass-formers [21–23]. We find that the patch-repetition analysis can be used to identify and characterise metastable states in this model, despite its trivial potential energy surface. However, the metastable states that are revealed absolutely require the time-averaging process described in [14]: in particular, there are states with a very broad spectrum of lifetimes, and the results of the patch-repetition analysis depend on the lifetime of the states under analysis. In this sense, the patch-repetition analysis is distinct from recent studies that aim to characterise amorphous order through analyses where a system is constrained (pinned) or biased to remain close to a typical reference configuration [24–27] – these analyses are purely static and have no dependence on the dynamical rules by which the system evolves. Such calculations therefore give trivial results for the East model, in contrast to the patch-repetition analysis.

We describe our models and methods in Sec. II before showing numerical results in Sec. III. We also identify a mapping between these states and configurations of an ideal gas of hard rods, where the size of the rods depends on the lifetime of the states. In Sec. IV, we discuss the implications of our results for studies of metastable states in general, and we also discuss connections between that analysis and recent work on large deviations of dynamical quantities in glassy systems [28–31]. Finally, we summarise our conclusions in Sec. V.

II. MODEL, METHODS, AND METASTABLE STATES

A. Model

The East model [17, 18] consists of L binary spins $n_i = 0, 1$, with $i = 1 \dots L$, and periodic boundaries. We refer to spins with $n_i = 1$ as ‘up’ and those with $n_i = 0$ as ‘down’. The notation $\mathcal{C} = (n_1, n_2, \dots, n_L)$ indicates a configuration of the system. The key feature of the model is that spin i may flip only if spin $i - 1$ is up. If this *kinetic constraint* [19, 20] is satisfied, spin i flips from 0 to 1 with rate c and from 1 to 0 with rate $1 - c$. We take $c/(1 - c) = e^{-\beta}$ where β is the inverse temperature, so small c corresponds to low temperature. The rates for spin flips obey detailed balance, so that the probability of configuration \mathcal{C} at equilibrium is simply $p^0(\mathcal{C}) = e^{-\beta \sum_i n_i} / Z$, where $Z = (1 + e^{-\beta})^L$ is the partition function. At equilibrium, one has $\langle n_i \rangle = c$, and the regime of interest is small c (low temperature).

Despite the trivial form of $p^0(\mathcal{C})$, the kinetic constraint in this model leads to complex co-operative dynamics at small c . In particular, the relaxation time of the model diverges in a super-Arrhenius fashion, as $\tau_0 \sim e^{\beta^2/(2 \ln 2)}$ [18, 33]. The rapid increase in relaxation time is illustrated in Fig. 1a where we show

$$C(t) = \frac{\langle n_i(t)n_i(0) \rangle - \langle n_i \rangle^2}{c(1 - c)}, \quad (1)$$

for various temperatures. The origin of the increasing time scale is a large set of metastable states, arranged hierarchically [18]: different states have different lifetimes which scale as c^{-b} . Here and throughout b is an integer which we use to classify the various relevant time scales in the system. Evidence for the separated timescales is shown in Fig. 1b: the correlation function decays via a sequence of plateaus that become more clearly separated as c is reduced.

B. Metastable states

To identify metastable states, we perform a time average over the spins, defining

$$\bar{n}_{it} = (1/t) \int_0^t dt' n_i(t'), \quad (2)$$

and a time-averaged spin profile

$$\bar{\mathcal{C}}_t = (\bar{n}_{1t}, \bar{n}_{2t}, \dots, \bar{n}_{Lt}). \quad (3)$$

The key observation of [14] is that if the system has metastable states indexed by $\alpha = 1, 2, \dots$, then each state is associated with a profile $\bar{\mathcal{C}}^\alpha$. Further, if t is much larger than the intrastate relaxation times, but small compared to their lifetimes, then the observed profile $\bar{\mathcal{C}}_t$ will almost surely be close to one of the $\bar{\mathcal{C}}^\alpha$. Hence, the

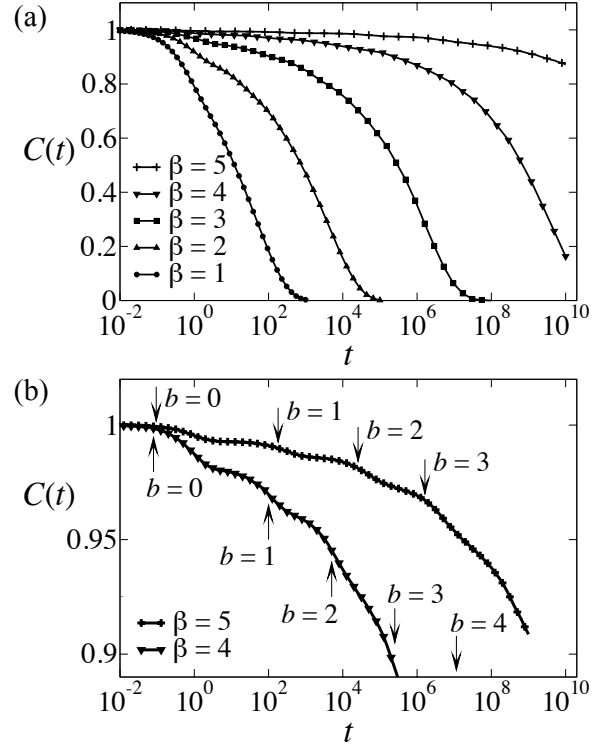


FIG. 1: Correlation function $C(t)$ in the East model. (a) The inverse temperature is varied from $\beta = 1$ to $\beta = 5$, showing a dramatic increase in relaxation time. (b) At the lowest temperatures, plateaus are apparent during the early stages of relaxation (where $C(t)$ is large). Arrows indicate the times for which data is shown in later figures. The behaviour at these times is representative of regimes $c^{1-b} \ll t \ll c^{-b}$: the rationale for choosing the specific values of t is discussed in the main text.

statistical properties of the (observable) profiles $\bar{\mathcal{C}}_t$ can be used to infer the properties of the metastable states in the system.

This situation, of many metastable states each associated with a profile $\bar{\mathcal{C}}^\alpha$, holds very accurately in the East model. As discussed by Sollich and Evans [18] (see also [34]), motion on a time scale $t \ll c^{-b} \ll \tau_0$ is restricted to domains of size 2^{b-1} , with each domain being immediately to the right of a long-lived up spin. Also, if $c^{1-b} \ll t \ll c^{-b}$ then spins within such domains typically flip many times within time t , while other spins are unlikely to flip at all. The result of this large number of flips is that $\bar{n}_{it} \rightarrow \langle n_i \rangle = c$ if spin i is within a mobile domain. Sollich and Evans [18] used the term ‘superdomain’ to describe these mobile domains. A metastable state with lifetime of order c^{-b} can be identified by specifying the position of its superdomains.

In terms of Fig. 1b, the limit $c^{1-b} \ll t \ll c^{-b}$ corresponds to choosing a time within a plateau of the correlation function. However, when using numerical results to gain information about metastable states, we

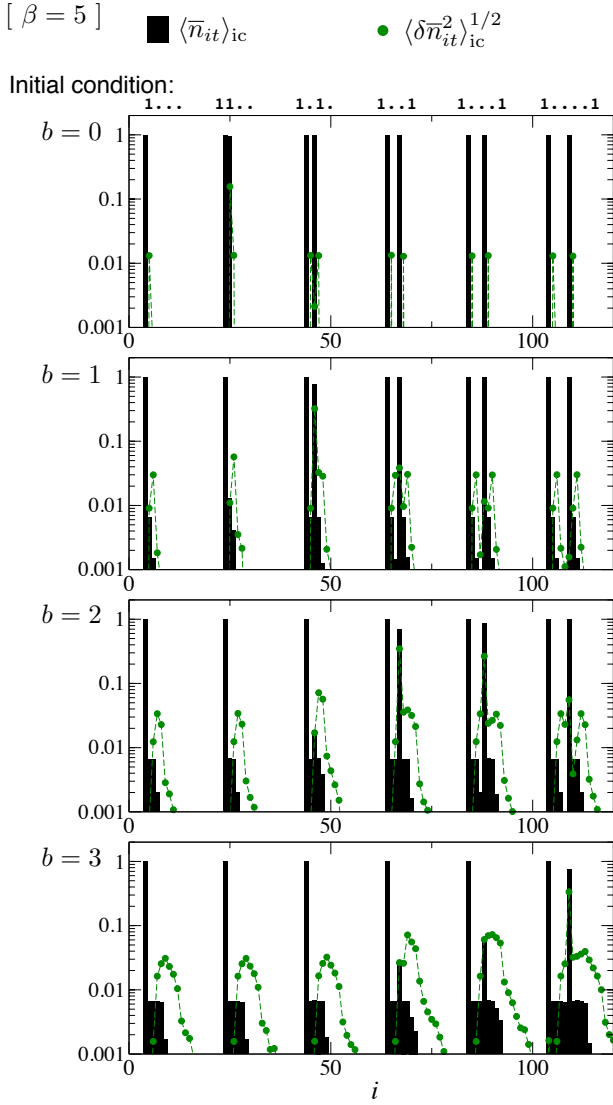


FIG. 2: Time averaged density profiles $\bar{\mathcal{C}}_t$ at $\beta = 5$ (so $c \approx 0.0067$). Averaging over many trajectories from the same initial condition, we show the mean profile $\langle \bar{n}_{it} \rangle_{ic}$ and its standard deviation $\langle (\delta \bar{n}_{it})^2 \rangle_{ic}$. The times correspond with the arrows in Fig. 1b, and are typical of the regimes $c^{1-b} \ll t \ll c^{-b}$. The approximate positions of the up spins in the initial condition are shown at the top of the figure (1s indicate up spins and dots indicate selected down spins). Typically, \bar{n}_{it} is either close to 1 (i.e., $\langle \bar{n}_{it} \rangle_{ic} \approx 1$ with $\langle (\delta \bar{n}_{it})^2 \rangle_{ic} \ll 1$) or \bar{n}_{it} is small (i.e., $\langle \bar{n}_{it} \rangle_{ic} \ll 1$ with $\langle (\delta \bar{n}_{it})^2 \rangle_{ic} \ll 1$). The separation between these two cases motivates the definition of the (coarse-grained) $\tilde{n}_{it} = 0, 1$.

find that saturating the limit $t \gg c^{1-b}$ is more important than $t \ll c^{-b}$: in the following we focus on the time points indicated by arrows in Fig. 1b, which correspond to $c^{1-b} \ll t \lesssim c^{-b}$. However, our results are similar if we use smaller times (as long as $t \gg c^{1-b}$).

To illustrate this behaviour, we have simulated trajec-

tories of the East model, starting from a particular initial condition that helps to reveal the physical processes at work. Fig. 2 shows the time-averaged spins $\langle \bar{n}_{it} \rangle_{ic}$ and their variances $\langle (\delta \bar{n}_{it})^2 \rangle_{ic}$, where the subscript “ic” indicates that the average was taken with a fixed initial condition (in contrast to other averages in this work which are conventional averages over equilibrium trajectories). We emphasise the following three points:

- All of the $\langle \bar{n}_{it} \rangle_{ic}$ are either close to 1 or of order $c \ll 1$. Also, the standard deviation $\langle (\delta \bar{n}_{it})^2 \rangle_{ic}^{1/2} \ll 1$ for all spins. Thus, for this initial condition and for each of these times t , one almost certainly finds a profile $\bar{\mathcal{C}}_t$ that is close to a reference profile $\bar{\mathcal{C}}_t^\alpha = \langle \bar{n}_{it} \rangle_{ic}$. Each reference profile (one for each value of t shown) can therefore be identified with a metastable state that is stable on a time scale t .
- For $b \geq 1$, any spins with $\langle \bar{n}_{it} \rangle_{ic} \approx 1$ are separated by at least 2^{b-1} spins with $\langle \bar{n}_{it} \rangle_{ic} \ll 1$. If two up spins are closer than this in the initial condition then the rightmost of them is within the mobile domain associated with the leftmost one. In that case, the rightmost spin (n_j) tends to flip many times and \bar{n}_{jt} converges to a value close to c .
- For this initial condition (and these time scales), the system relaxes independently in each of 6 independent regions. This means that the dynamical evolution of separate patches of the system can be treated independently.

These three points establish the central requirements for our analysis of metastable states. The first shows that the metastable states in this system are well-defined, while the second shows that metastable states with different lifetimes have different internal structures. The third point establishes that one may decompose the behaviour of the system into independent regions, at least for this initial condition. Building on this point, Fig. 3 shows how the local behaviour evolves with time, for various different initial conditions (the predictions shown follow from the superspin analysis of [18] and are also consistent with our numerical results). We note that while some initial conditions belong to a single metastable state (and always yield the same time-averaged profile $\bar{\mathcal{C}}_t$), there are other initial conditions that exist on the border between states (and therefore may yield one of several profiles). For these cases, it will not be true that $\langle (\delta \bar{n}_{it})^2 \rangle_{ic}^{1/2} \ll 1$, but it is true that for typical trajectories, $\bar{\mathcal{C}}_t \approx \bar{\mathcal{C}}_t^\alpha$ for some metastable state α .

In general, the analysis of Kurchan and Laloux [35] indicates that typical configurations of any large finite-dimensional system always lie on a border between states. For the East model, this result follows from the observation that the local configuration 111... will occur many times in a large system: in the regions where this occurs, the system may relax into one of two averaged profiles [either 1x1x... or 1xx..., (see Fig. 3)]. Hence a typical configuration of the system cannot be associated to a single

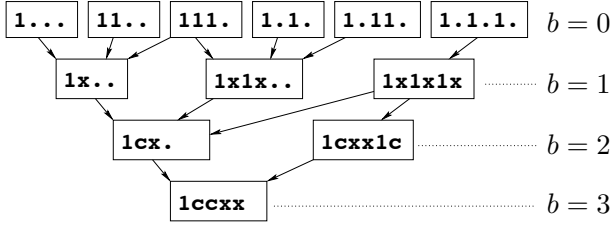


FIG. 3: Schematic illustration of time evolution among metastable states. Each box represents a state, labelled by its characteristic local density profile, and a value of b that indicates its lifetime (of order c^{-b}). To describe the profile we use a notation suggested by Fig. 2, based on the relative sizes of $\langle \bar{n}_{it} \rangle_{ic}$ and $\langle \delta \bar{n}_{it}^2 \rangle_{ic}^{1/2}$. We distinguish four cases: (i) a 1 represents a spin with $\bar{n}_{it} \approx 1$ (up to a tolerance much less than 1); (ii) a dot represents a spin with $\bar{n}_{it} \ll c$; (iii) a c represents a spin with $\bar{n}_{it} \approx c$ (up to a tolerance much less than c); (iv) an x represents a spin with $\bar{n}_{it} \sim c$ (that is, a typical value c with a tolerance much less than 1 but bigger than c). The 1 corresponds to $\tilde{n}_{it} = 1$ while x, c and dot all correspond to $\tilde{n}_{it} = 0$. Arrows indicate how a profile on one time scale evolves into a different profile after averaging over a longer time scale. Some states have more than one outward arrow, indicating that they may evolve into one of several possible profiles, so they are on a borderline between the various (more stable) states into which they may evolve.

averaged profile. However, a key insight from [14] is that while it is not possible to establish a one-to-one mapping between initial conditions and metastable states, it is possible to establish such a mapping between profiles $\bar{\mathcal{C}}_t$ and metastable states.

C. Methods for counting metastable states

We now turn to the patch-repetition analysis proposed by Kurchan and Levine [14] as a method for analysis of metastable states. We wish to consider the probability distribution of profiles $\bar{\mathcal{C}}_t$, since these are in one-to-one correspondence with metastable states. In general, the averages \bar{n}_{it} have continuous values, and a tolerance ϵ is required [14] in order to identify if a state $\bar{\mathcal{C}}_t$ is “close” to a reference profile $\bar{\mathcal{C}}_t^\alpha$. However, in the East model, we have $\bar{n}_{it} \approx 0, 1$ (recall Fig. 2) so we define

$$\tilde{n}_{it} = \Theta(\bar{n}_{i,t} - a), \quad (4)$$

where $\Theta(x)$ is a step function, and the threshold $a = 1/2$ (results depend weakly on this threshold). We then obtain a binary profile

$$\tilde{\mathcal{C}}_t = (\tilde{n}_{1t}, \tilde{n}_{2t}, \dots, \tilde{n}_{Lt}), \quad (5)$$

and we consider the statistical properties of these profiles, as a proxy for the $\bar{\mathcal{C}}_t$.

To analyse the distribution over the $\tilde{\mathcal{C}}_t$, we use the patch-repetition analysis [14]. To this end, consider a patch of the system of size ℓ , for example $\mathcal{B}_i^\ell = (\tilde{n}_{it}, \tilde{n}_{i+1,t}, \dots, \tilde{n}_{i+\ell-1,t})$. Then, for a large system, one evaluates

$$S_{\ell,t} = - \sum_{\mathcal{B}^\ell} [n(\mathcal{B}^\ell)/L] \log [n(\mathcal{B}^\ell)/L] \quad (6)$$

where $n(\mathcal{B}^\ell)$ is the number of occurrences of patch \mathcal{B}^ℓ in $\tilde{\mathcal{C}}_t$, and the sum runs over all patches of size ℓ that appear in $\tilde{\mathcal{C}}_t$. (Clearly $\sum_{\mathcal{B}^\ell} n(\mathcal{B}^\ell) = L$ since the total number of patches is L .)

As long as correlations in the system are of finite range, one may define the entropy density associated with the profiles $\tilde{\mathcal{C}}_t$ as

$$\mathcal{S}_t = \lim_{\ell \rightarrow \infty} S_{\ell,t}/\ell. \quad (7)$$

Since we expect a one-to-one correspondence between profiles $\tilde{\mathcal{C}}_t$ and metastable states of lifetime at least t , then we can identify \mathcal{S}_t as the entropy density associated with these metastable states. The (extensive) quantity $L\mathcal{S}_t$ is sometimes called the “complexity” [11, 12, 14] (although we emphasise that we are working with states of fixed finite lifetime, not the infinitely long-lived states that exist in mean-field models).

III. PATCH-REPETITION ANALYSIS AND DYNAMICAL CORRELATIONS

We now present numerical results that illustrate how the patch repetition analysis is effective in identifying and characterising metastable states in the East model, and how the results of this analysis can be used to predict dynamical correlation functions. These results illustrate the operation of the scheme, and the central role played by the averaging time t . The implications of these results for other glassy systems will be discussed in the following Section.

In the East model, we have evaluated $S_{\ell,t}$ numerically for the times t shown with arrows in Fig. 1b. Fig. 4 shows our results (symbols), which we present by plotting $S_{\ell+1,t} - S_{\ell,t}$ as a function of ℓ . We first observe that for $t \ll 1$ (i.e., $b = 0$), then $S_{\ell+1,t} - S_{\ell,t}$ is independent of ℓ . This result follows immediately from the trivial equilibrium distribution $p^0(\mathcal{C})$ in the East model. However, on averaging over larger time scales, structure appears in these entropy measurements, and one may easily identify a length scale ℓ^* associated with convergence of $S_{\ell+1,t} - S_{\ell,t}$ to its large- ℓ limit \mathcal{S}_t .

To account for the ℓ -dependence of $S_{\ell,t}$, recall that the “superdomain” argument of [18] indicates that sites with $\tilde{n}_{it} = 1$ are separated by at least 2^{b-1} lattice sites (for $b \geq 1$). This rule indicates that the statistics of the time-averaged profiles $\tilde{\mathcal{C}}_t$ are related to those of systems of hard rods of length $m = 1 + 2^{b-1}$. In fact, for times much less than τ_0 , we find that the statistics of the profiles $\tilde{\mathcal{C}}_t$ are

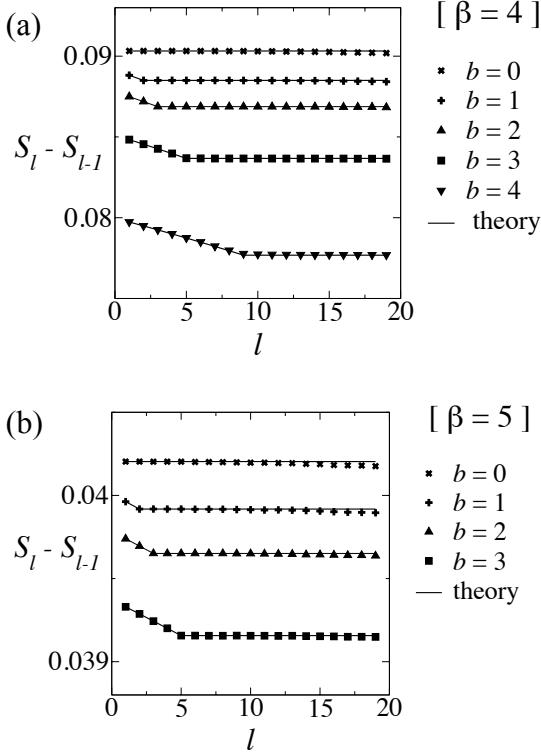


FIG. 4: Patch entropies $S_{\ell,t}$ (points) associated with the density profiles \tilde{n}_{it} , evaluated at the times indicated in Fig. 1b and for (a) $\beta = 4$ and (b) $\beta = 5$. The ‘theory’ lines are the predictions of (8,9), where the density ρ is obtained as $\langle \tilde{n}_{it} \rangle$ and the rod length $m = 1 + 2^{b-1}$ (or $m = 1$ for $b = 0$).

almost exactly those of an ideal gas of hard rods of length m , where the leftmost site of each hard rod carries a ‘1’ and all others site carry a ‘0’. If the number density of rods is ρ , straightforward counting arguments show that the patch entropies for this hard rod system are given by

$$S_{\ell}(m, \rho) = -\ell \rho \log \rho - (1 - \ell \rho) \log(1 - \ell \rho), \quad \ell \leq m, \quad (8)$$

and

$$S_{\ell}(m, \rho) = S_m(m, \rho) + (\ell - m) \mathcal{S}^{\text{rod}}(m, \rho), \quad \ell > m, \quad (9)$$

where

$$\mathcal{S}^{\text{rod}}(m, \rho) = -\rho \log \rho - (1 - m\rho) \log(1 - m\rho) + [1 - (m-1)\rho] \log[1 - (m-1)\rho] \quad (10)$$

is the total entropy density.

The predictions of (8) and (9) are shown in Fig. 4 as solid lines. The fit is excellent. The value of ρ has been calculated from the numerical data (as $\rho = \langle \tilde{n}_{it} \rangle$), but no other fit parameters are required (we take $m = 1 + 2^{b-1}$). We conclude that metastable states in the East model with lifetimes $t \sim c^{-b}$ are in one-to-one correspondence with configurations of hard rods of length $1 + 2^{b-1}$. At equilibrium, states with equal numbers of rods are

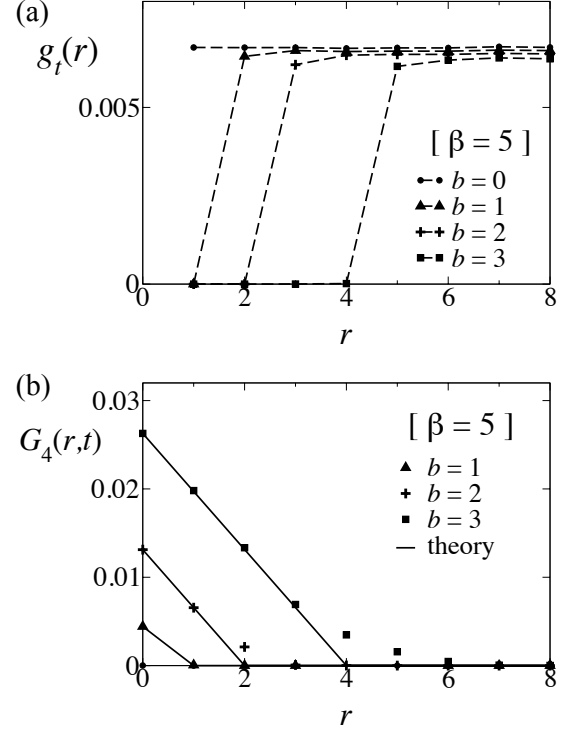


FIG. 5: Spatial correlation functions at $\beta = 5$ and times indicated in Fig. 1b. (a) Two-point correlations $g_t(r)$ of the time-averaged density \bar{n}_{it} . The dashed lines are guides to the eye. The mapping to hard rods indicates that $g_t(r)$ should be equal to 0 for $r \leq 2^{b-1}$ and constant ($= \rho$) otherwise, consistent with the data. (b) Two-point correlations $G_4(r, t)$ of the persistence function p_{it} . The ‘theory’ lines are predictions of (13), where ρ is fitted to the value $G_4(0, t)$.

equiprobable, and the number density of such hard rods is $\rho \approx c$. (To be precise, for $t \ll t_0$ then $\rho = c - O(c^2)$: one has $\langle \tilde{n}_{it} \rangle = c$, but the coarse-graining procedure leading to \tilde{n}_{it} means that the average number of sites with $\tilde{n}_{it} = 1$ is less than the average number of sites with $n_i = 1$.) It is however useful to recall at this point that we have always been restricting our analysis to the situation $c^{-b} \ll \tau_0$, which also implies that $m\rho \ll 1$ (recall τ_0 is the bulk relaxation time). For times of order τ_0 , the situation is more complicated, since time scales are no longer well-separated [32]. To the extent that that metastable states exist on these time scales, we expect them still to be in one-to-one correspondence with hard-rod configurations, but states with equal numbers of rods are no longer equiprobable. The same limitations mean that the superdomain analysis of [18] does not give quantitative results for structural relaxation at equilibrium.

Fig. 5 shows the correlation function between time-averaged densities

$$g_t(r) = \frac{\langle \bar{n}_{it} \bar{n}_{i+r,t} \rangle}{\langle \bar{n}_{it} \rangle}. \quad (11)$$

Given that the distribution over metastable states is that of uncorrelated hard rods, one expects that $g_t(r) \approx 0$ for $1 \leq r \leq 2^{b-1}$ and $g_t(r) \approx \rho$ for $r > 2^{b-1}$. This is confirmed numerically in Fig. 5(a).

Fig. 5(b) shows the correlation between single-site “persistences”

$$G_4(r, t) = \langle p_{it} p_{i+r, t} \rangle - \langle p_{it} \rangle^2, \quad (12)$$

where the persistence $p_{it} = 1$ if spin i does not flip at all between times 0 and t ; otherwise $p_{it} = 0$. Based on the superspin picture, we assume that relaxation within states is the only motion possible on times less than t , so all sites should have $p_{it} = 1$, except that each up spin in \tilde{C}_t is followed by 2^{b-1} spins with $p_{it} = 0$.

Assuming that this picture holds, one arrives (for $c^{1-b} \ll t \ll c^{-b}$) at

$$G_4(r, t) = \max[\rho(1 - r/2^{b-1}), 0] \quad (13)$$

where ρ is the number density of hard rods discussed above. Comparing this prediction with the numerical data of Fig. 5b, the agreement is reasonable, but there are significant deviations. The data for $G_4(r, t)$ indicate that blocks of more than 2^{b-1} spins with $p_{it} = 0$ occur more often than expected. This occurs because the persistence p_{it} is sensitive to (atypical) flips of spin i that may occur even if this spin is not within a mobile domain. Such flips tend to occur to the right of mobile domains, increasing their apparent size. On the other hand, the time-averaged density \bar{n}_{it} is less sensitive to such rare spin flips: a significant deviation of \bar{n}_{it} from its typical behaviour requires that n_i deviates from its typical behaviour for a time comparable with t . This emphasises the effectiveness of the time-averaged spin \bar{n}_{it} as a good measurement for probing metastable states, while the persistence p_{it} is less effective for this.

IV. DISCUSSION OF METASTABLE STATES

A. Length scales

A central aim of [14] was to identify a length scale (or perhaps several length scales) associated with “amorphous order”. It is clear from Figs. 4 and 5 that for times $t \sim c^{-b}$, there is a length scale $\ell^* \simeq 2^{b-1}$ associated with the metastable states in the East model. In general, this length scale should reflect structural features associated with metastable states of lifetime t . Here, this is simply the minimal possible spacing between spins with $\tilde{n}_{it} = 1$. The longer-lived the states, the larger is ℓ^* , and the greater the degree of internal structure within the states.

While these states can only be obtained by a dynamical construction (the time averaging of the spin profile), we note that they do have static structure, as measured (for example) by $g_t(r)$. Hence, one may explain properties of

the system by a ‘free energy landscape’ metaphor, of activated hopping amongst states (basins), with each state having a distinct local structure. The (time-dependent) length ℓ^* also matches the length scale ξ_4 associated with dynamical heterogeneity in the model, which is usually measured (in the East model) by the persistence correlation function $G_4(r, t)$. The general inference here that is that the time-averaging procedure used to determine ℓ^* will lead to coupling between ℓ^* and dynamical heterogeneities associated with intra-state (relatively fast) dynamical motion.

We note that the length scale ℓ^* is obtained by considering the approach of $S_{\ell+1, t} - S_{\ell, t}$ to its large- ℓ limit S_ℓ : an alternative route [14, 16] is to expand the entropy for large ℓ as $S_\ell = S \ell^d [1 + (\xi/\ell)^{\nu-d} + \dots]$ where d is the spatial dimension, ξ a characteristic length scale, and ν a scaling exponent. Calculating results for the East model based on the hard rod analysis, we have $d = 1$ and $\nu = 0$: the resulting length scale is $\xi = \ell^* (\ell^* S_{\ell=1} - S_{\ell^*}) / (2S_{\ell^*})$. As may be inferred from Fig. 4, the entropy difference $\ell^* S_{\ell=1} - S_{\ell^*}$, is small compared to S_{ℓ^*} , meaning that $\xi \ll \ell^*$. The interpretation of ξ is therefore not clear in this case: it would be more appropriate to write $S_\ell = S \ell^d [1 + a(\xi/\ell)^{\nu-d} + \dots]$ where a is an amplitude (small in this case), and $\xi \approx \ell^*$ the true length scale. However, extraction the determination of two parameters a and ξ makes this method non-trivial [in this case one might take $a = (S_{\ell=1}/S) - 1$ but it is not clear that this is the best choice in general].

Another length scale [14] that can be extracted from S_ℓ is the length ℓ_1 for which $S_\ell \approx 1$. In this model, $\ell_1 \sim 1/|c \log c|$, comparable (but not equal to) the typical distance $(1/c)$ between up spins. However, the length scale ℓ_1 does not play any obvious role in the behaviour of the system. A similar conclusion was found in [16]. However, contrary to the models considered in [16], we find that S_ℓ/ℓ approaches its large- ℓ limit from above in this model, and not from below. We do not have any simple physical argument for this observation, although we do note that the total entropy of the East is very small at low temperatures, since the model does not account for the diversity of possible “inactive” states that are commonly found in glassy systems [36, 37].

The conclusion of this analysis is that the ℓ -dependence of S_ℓ does encode considerable information about the range of correlations an amorphous system. For the East model, it is relatively simple to identify the relevant physical length scale as ℓ^* , but more generally, it remains unclear how to interpret measurements of S_ℓ . Certainly, the subtleties associated with this interpretation should be borne in mind in future studies.

B. Atypical states and the complexity $\Sigma(f)$

We established in Sec. III that the metastable states in the East model are in correspondence with configurations of hard rods. At equilibrium, the system typically

occupies states whose number density of rods is $\rho \sim c$. However, as discussed in [14], it may be useful to consider ensembles in which the model is biased into atypical metastable states (for example, with higher or lower values of ρ).

We define a free energy density for state α by writing the probability that the system is in that state as

$$P(\alpha) = e^{-\beta L f_\alpha} / Z, \quad (14)$$

where Z is the usual equilibrium partition function of the system. Based on the mapping to hard rods, we have $f_\alpha = -\mu \mathcal{N}_\alpha$ where μ is a (negative) chemical potential, and \mathcal{N}_α is the number density of up spins in $\tilde{\mathcal{C}}^\alpha$ (i.e., the number density of rods). For a given average density ρ , the chemical potential μ may be obtained as $\beta\mu = -\frac{\partial}{\partial \rho} \mathcal{S}^{\text{rod}}(m, \rho)$.

Now consider a modified ensemble in which states occur with probability

$$P_q(\alpha) = e^{-\beta q L f_\alpha} / \mathcal{Z}(q) \quad (15)$$

with $\mathcal{Z}(q) = \sum_\alpha e^{-\beta q L f_\alpha}$. The ensemble with $q = 1$ corresponds to equilibrium: for large q then states with more rods are suppressed while for $q < 1$ they are enhanced. As $q \rightarrow 0$, all states are equiprobable so the ensemble is dominated by the most numerous states (those with the highest entropy).

Since the probability of state α depends on q through the exponential of an extensive quantity, the modified ensemble of (15) is dominated by states that are very rare at equilibrium: such ensembles are the subject of large deviation theory [38]. To investigate the properties of this ensemble, it is useful to consider the average free energy of states within the modified ensemble:

$$f(q) = \sum_\alpha f_\alpha P_q(\alpha) = -\frac{1}{\beta L} \frac{\partial}{\partial q} \log \mathcal{Z}(q). \quad (16)$$

Now rewrite the definition of $\mathcal{Z}(q)$ as

$$\mathcal{Z}(q) = \int df e^{\Sigma(f) - \beta q L f} \quad (17)$$

where (by definition) $e^{\Sigma(f)}$ is the density of states with free energy f , so $\Sigma(f)$ is the (extensive) complexity [12, 14]. For the East model, recall that the free energy $f_\alpha = -\mu \mathcal{N}_\alpha$, and the density of states with a given number of rods is $e^{L \mathcal{S}^{\text{rod}}(m, \rho)}$ [recall (10)]. Thus, for the East model, we have a concrete expression for the complexity:

$$\Sigma_t(f) = L \mathcal{S}^{\text{rod}}(m_t, -f/\mu_t), \quad (18)$$

where μ_t is the rod chemical potential and m_t is the relevant rod length; we have reintroduced the subscript t as a reminder that we are counting metastable states with lifetime much greater than some fixed time t , and that the rod size m and chemical potential μ depend on this time.

It follows from (17) that the modified ensemble of (15) maps to an ensemble of hard rod configurations whose chemical potential is $q\mu$ (here $\mu < 0$ is the rod chemical potential of the equilibrium ensemble with $q = 1$). As q is reduced (the chemical potential becomes less negative), the number of hard rods increases. As $q \rightarrow 0$, one finds the maximum entropy state, $\rho = 1/(m+1)$; continuing to negative q , the system approaches the maximal density state $\rho = 1/m$. For $q > 1$, the number of rods decreases, with $\rho \rightarrow 0$ (and therefore $f \rightarrow 0$) as $q \rightarrow \infty$. The large- q limit is similar to the entropy crises found in mean-field models [12], except that $\Sigma(f) \rightarrow 0$ with a diverging gradient $d\Sigma/df \rightarrow \infty$: this is the reason that the transition takes place as $q \rightarrow \infty$ [14]. In summary, we find that $f(q)$ is a smooth function of q , with singular behaviour only as $q \rightarrow \pm\infty$. This means that phase transitions only occur at zero temperature, as expected in the East model [19, 20].

C. Biased ensembles based on patches and the role of dynamical fluctuations

In the previous subsection, we analysed atypical states in the East model using the superspin picture of [18] and the numerical results that we obtained for typical states. Kurchan and Levine [14] proposed a method for numerical investigation of atypical states, via the ensemble (15). However, numerical sampling of such biased ensembles is difficult, since these ensembles are dominated by configurations that are far from typical. In the remainder of this Section we analyse different methods for analysing rare metastable states. We use the East model as a representative example, but the main aspects of the discussion apply quite generally to models with many metastable states.

The method proposed in [14] for analysis of atypical states was based on Renyi complexities (see for example [39]): the idea is that one estimates a quantity $Y_{\mathcal{B}}$ that can be used to infer the free energy associated with a patch \mathcal{B} of size ℓ . Each possible patch has a free energy density that is estimated as $Y_{\mathcal{B}} = (-1/\ell) \log[n(\mathcal{B})/L]$ where $n(\mathcal{B})$ is the number of times that patch \mathcal{B} appears in $\tilde{\mathcal{C}}_t$ [recall (6)]. Writing $n(\mathcal{B})/L = e^{-\ell Y_{\mathcal{B}}}$ and comparing with (14) motivates the analogy between $Y_{\mathcal{B}}$ and the free energy density βf_α .

Then, one may analyse the q -ensemble by giving extra statistical weight to patches with large (or small) values of Y . That is, consider a patch-analogue of (15) where one assigns patch probabilities:

$$p_q(\mathcal{B}) = \frac{e^{-q\ell Y_{\mathcal{B}}}}{\mathcal{Z}_p(q)} \quad (19)$$

with $\mathcal{Z}_p(q) = \sum_{\mathcal{B}} e^{-q\ell Y_{\mathcal{B}}}$. Since $Y_{\mathcal{B}}$ can be estimated directly via $n(\mathcal{B})$, one may also estimate a free-energy-

like quantity, which is the Renyi complexity:

$$K_{q,\ell} = \frac{1}{\ell(q-1)} \log \sum_{\mathcal{B}} e^{-q\ell Y_{\mathcal{B}}} \\ = \frac{1}{\ell(q-1)} \log \sum_{\mathcal{B}} [n(\mathcal{B})/L]^q. \quad (20)$$

The patch quantity $(q-1)K_{q,\ell}$ is analogous to the quantity $(1/L) \log \mathcal{Z}(q)$, defined for states in the previous section. For large enough ℓ , one expects the modified ensemble defined by (19) to resemble that defined by (15).

From a numerical perspective, this approach is difficult – one is attempting to reconstruct a biased ensemble using data from an equilibrium one, and typical configurations from the two ensembles are quite different from one another. The usual approach to this problem is to use a biased sampling scheme such as umbrella sampling [40] for ensembles of configurations, or transition path sampling [41] for ensembles of trajectories. Here the situation is subtle: while the bias in (15) appears to be a configurational one, based on free energies of states, we recall that any practical sampling scheme uses *time-averaged* profiles to infer the relevant states. This means that patches that are rare in (20) may be associated with unusual metastable states, or they may be associated with rare dynamical events in which the averaged profile $\bar{\mathcal{C}}_t$ does not converge to any of the profiles $\bar{\mathcal{C}}_t^\alpha$ that are associated with metastable states in the system. This motivates us to consider the relation to dynamical sampling methods and recent work on dynamical large deviations.

D. Relation to dynamical large deviations

The statistical properties of *time-integrated* dynamical quantities have received considerable interest recently, especially through studies of large deviations in glassy systems [28–31, 42–45] (including the East model [28, 29, 45]). The most relevant situation for this work is the one considered for a spin-glass model in [31], where the time t (there called t_{obs}) is well-separated from both a fast (intra-state) relaxation time scale t_f and a slow (inter-state) relaxation time t_s . The question of interest there is: given a quantity $k(\mathcal{C})$ that can be evaluated for a given configuration, what is the probability distribution of $K = \int_0^t k(\mathcal{C}(t')) dt'$? Clearly, this is closely related to distributions of the quantities considered here, such as $\bar{n}_{it} = (1/t) \int_0^t n_i(t') dt'$. We note that in [31], the *fast* time scale t_f was comparable with the equilibrium relaxation time of the system, while the *slow* time scale was much longer still. Here we consider the case where $t_f \ll t \ll t_s \ll \tau_0$: for example $t_f = c^{1-b}$ and $t_s = c^{-b}$, as above. Nevertheless, the main results of [31] apply also in this case.

In particular, one may consider a biased ensemble where a dynamical trajectory $\mathcal{C}(t)$ occurs with probabil-

ity

$$\text{Prob}[\mathcal{C}(t)|s] = \text{Prob}[\mathcal{C}(t)|0] \cdot e^{-sK[\mathcal{C}(t)]} \cdot \frac{1}{Z_d(s)}. \quad (21)$$

Here, the short-hand notation $[\mathcal{C}(t)]$ indicates dependence on a trajectory of the system (with time running from 0 to t), while $\text{Prob}[\mathcal{C}(t)|0]$ is the probability of trajectory $\mathcal{C}(t)$ at equilibrium, and $Z_d(s)$ is a normalisation constant. Following [31], in the joint limit $t_f \ll t \ll t_s$, this biased ensemble develops a singular dependence on s . That is, if the average value of k within state α is k_α then for $s > 0$ the ensemble is dominated by the metastable state(s) with minimal k_α , while for $s < 0$ it is dominated by state(s) with maximal k_α .

If one replaces $s \rightarrow \lambda/t$ in (21), one sees that trajectories are now being biased according to their average values of $k(\mathcal{C})$ (instead of their integrated value). Assuming that dynamical fluctuations can be neglected (that is, $\bar{\mathcal{C}}_t \approx \bar{\mathcal{C}}^\alpha$, due to separation of time scales), and that every trajectory is localised in a single metastable state, one arrives at

$$\text{Prob}[\mathcal{C}(t)|s] \approx \text{Prob}[\mathcal{C}(t)|0] \cdot e^{-\lambda k_\alpha[\mathcal{C}(t)]} \cdot \frac{1}{Z_d(\lambda/t)} \quad (22)$$

where $\alpha[\mathcal{C}(t)]$ is the state within which $\mathcal{C}(t)$ is localised. In that case, one may write the probability of state α as

$$P_\lambda(\alpha) \approx e^{-\beta L f_\alpha} \cdot e^{-\lambda k_\alpha} \cdot \frac{1}{Z_s(\lambda)} \quad (23)$$

where $Z_s(\lambda)$ is a normalisation constant. Physically, (23) indicates that the effect of weak bias $s = O(1/t)$ in (21) is to reshuffle probability between metastable states, in a similar way to that anticipated in (15). One may also conjecture that the singular dependence of the ensemble in (21) on the parameter s might be resolved as a smooth change on a scale $s = O(1/t)$. (Note however that this behaviour would still be far beyond any linear-response regime.)

Further, if $k(\mathcal{C})$ can be chosen so that $k_\alpha \approx \beta L f_\alpha$, then (23) reduces to (15), with $\lambda = q - 1$. That would allow the ensemble of (15) to be sampled via the numerical methods that have been used already to sample the s -ensemble. In fact this is a relatively simple matter in the East model, since $f_\alpha = -\mu \mathcal{N}_\alpha$ is tightly correlated with the total density of up spins $L^{-1} \sum_i n_i$, whose large deviations were considered in [28]. However, the construction required to obtain the statistics of metastable states is different from that used in most s -ensemble studies so far, since it would require analysis of trajectories with $1 \ll t \ll \tau_{\text{eq}}$ using $s = O(1/t)$ (where τ_{eq} is the structural relaxation time): previous studies concentrated on the alternative limit $s = O(1)$ and $t \gg \tau_{\text{eq}}$. The role of dynamical fluctuations also needs careful consideration when comparing results: we are assuming here that $\bar{\mathcal{C}}_t$ is always close to the relevant $\bar{\mathcal{C}}^\alpha$ but ensuring that this is indeed the case for trajectories in the s -ensemble requires careful examination of the limit $t_f \ll t \ll t_s$.

Finally, we recall that for non-zero c , the East model has a phase transition in the s -ensemble, in the limit where $t \gg \tau_0$ [29]. (This is distinct from possible singular behaviour if $c^{1-b} \ll t \ll c^{-b}$ which clearly requires $c \rightarrow 0$.) It is clear from [28, 46] that this transition is associated with a “phase-separated” regime where time-averaged profiles become macroscopically inhomogeneous, containing a large “bubble”, free of excitations. In the language of hard rods, this bubble corresponds to a large rod (length m of the same order as the system size), with a commensurately long lifetime (diverging with the system size). In general, if states with very long lifetimes exist, one expects them to dominate the system for $s > 0$ and $t \rightarrow \infty$: the necessary link [14] between the very long lifetime and a diverging length scale is particularly clear KCMs such as the East model [29].

V. CONCLUSION AND OUTLOOK

We have shown that the patch-repetition analysis of Kurchan and Levine [14] is useful in identifying metastable states in the East model, and analysing their structure. The results are consistent with the analysis of Sollich and Evans [18], as shown by the excellent fits in Fig. 4. Knowledge of the metastable states can also be used to predict dynamical correlation functions as shown in Fig. 5.

We have emphasised that the patch-repetition analysis is inherently dynamical in nature, because of its construction from time-averaged density profiles. In this sense, it can be used to identify metastable states even in systems where the potential energy landscape is flat and featureless. (This observation can also be rationalised through the idea that the flat landscape is endowed with a non-trivial metric [47], encapsulating the idea that motion within some regions of the landscape may be much faster than motion between those regions.)

Finally, we compared several different ways of analysing the distribution of metastable states within a system, through biased ensembles in which patch probabilities are reweighted (19) and through ensembles where trajectories are biased by some time-averaged measure (21). In the end, these methods for numerical analysis of metastable states must be tested on atomistic models, to understand how efficient they are and how useful their results will be. We hope that future studies in this area will be forthcoming.

Acknowledgments

I would like to thank Jorge Kurchan, Peter Sollich, and Giulio Biroli, for enlightening discussions on metastable states, patches and large deviations. This work was funded by the EPSRC through grant EP/I003797/1.

-
- [1] M. D. Ediger, C. A. Angell and S. R. Nagel, *J. Phys. Chem.* **100**, 13200 (1996).
 - [2] P. G. Debenedetti and F. H. Stillinger, *Nature* **410**, 259 (2001)
 - [3] J. P. Garrahan and D. Chandler, *Phys. Rev. Lett.* **89**, 035704 (2002); J. P. Garrahan and D. Chandler, *Proc. Nat. Acad. Sci. USA* **100**, 9710 (2003).
 - [4] D. Chandler and J. P. Garrahan, *Ann. Rev. Phys. Chem.* **61**, 191 (2010).
 - [5] M. L. Manning and A. J. Liu, *Phys. Rev. Lett.* **107**, 108302 (2011)
 - [6] M. Goldstein, *J. Chem. Phys.* **51**, 3728 (1969).
 - [7] A. Heuer, *J. Phys.: Cond. Matt.* **20**, 373101 (2008)
 - [8] T. R. Kirkpatrick, D. Thirumalai and P. G. Wolynes, *Phys. Rev. A* **40**, 1045 (1989).
 - [9] J. Bouchaud and G. Biroli, *J. Chem. Phys.* **121**, 7347 (2004).
 - [10] A. S. Keys, L. O. Hedges, J. P. Garrahan, S. C. Glotzer and D. Chandler, *Phys. Rev. X* **1**, 021013 (2011).
 - [11] D. J. Thouless, P. W. Anderson and R. Palmer, *Phil. Mag.* **35**, 593 (1977).
 - [12] T. Castellani and A. Cavagna, *J. Stat. Mech* (2005) P05012.
 - [13] G. Biroli and J. Kurchan, *Phys. Rev. E* **64**, 016101 (2001).
 - [14] J. Kurchan and D. Levine, *J. Phys. A* **44**, 035001 (2011).
 - [15] F. Sausset and D. Levine, *Phys. Rev. Lett.* **107**, 045501 (2011).
 - [16] C. Cammarota and G. Biroli, *EPL* **98**, 36005 (2012).
 - [17] J. Jäckle and S. Eisinger, *Z. Phys. B* **84**, 115 (1991).
 - [18] P. Sollich and M. R. Evans, *Phys. Rev. Lett.* **83**, 3238 (1999); *Phys. Rev. E* **68**, 031504 (2003).
 - [19] F. Ritort and P. Sollich, *Adv. Phys.* **52**, 219 (2003).
 - [20] J. P. Garrahan, P. Sollich and C. Toninelli, Ch. 10 in *Dynamical heterogeneities in glasses, colloids and granular media*, eds: L. Berthier, G. Biroli, J.-P. Bouchaud, L. Cipelletti and W. van Saarloos (OUP, Oxford UK).
 - [21] L. Berthier and J. P. Garrahan, *J. Phys. Chem. B* **109**, 3578 (2005);
 - [22] Y. S. Elmatad, D. Chandler and J. P. Garrahan, *J. Phys. Chem. B* **113**, 5563 (2009).
 - [23] A. S. Keys, J. P. Garrahan and D. Chandler, *Proc. Acad. Nat. Sci. USA* **110**, 4482 (2013).
 - [24] C. Cammarota and G. Biroli, *Proc. Nat. Acad. Sci. USA* **109**, 8850 (2012)
 - [25] W. Kob and L. Berthier, *Phys. Rev. Lett.* **110**, 245702 (2013).
 - [26] R. L. Jack and L. Berthier, *Phys. Rev. E* **85**, 021120 (2012)
 - [27] L. Berthier, *Phys. Rev. E* **88**, 022313 (2013).
 - [28] M. Merolle, J.P. Garrahan and D. Chandler, *Proc. Natl. Acad. Sci. USA* **102**, 10837 (2005).
 - [29] J. P. Garrahan, R. L. Jack, V. Lecomte, E. Pitard, K. van Duijvendijk and F. van Wijland, *Phys. Rev. Lett.* **98**, 195702 (2007); *J. Phys. A* **42**, 075007 (2009).
 - [30] L. O. Hedges, R. L. Jack, J. P. Garrahan and D. Chandler, *Science* **323**, 1309 (2009).
 - [31] R. L. Jack and J. P. Garrahan, *Phys. Rev. E* **81**, 011111

- (2010).
- [32] P. Chleboun, A. Faggionato, F. Martinelli, arXiv:1212.2399.
 - [33] N. Cancrini, F. Martinelli, C. Roberto and C. Toninelli, J. Stat. Mech. (2007) L03001
 - [34] D. Aldous and P. Diaconis, J. Stat. Phys. **107**, 945 (2002).
 - [35] J. Kurchan and L. Laloux, J. Phys. A **29**, 1929 (1996)
 - [36] G. Biroli, J.-P. Bouchaud, and G. Tarjus, J. Chem. Phys. **123**, 044510 (2005).
 - [37] D. Chandler and J. P. Garrahan, J. Chem. Phys. **123**, 044511 (2005).
 - [38] H. Touchette, Phys. Rep. **478**, 1 (2009).
 - [39] G. Paladin and A. Vulpiani, J. Phys. A **19**, L997 (1986).
 - [40] D. Frenkel and B. Smit, *Understanding Molecular Simulation*, 2nd edition (Academic Press, 2001).
 - [41] P. Bolhuis, D. Chandler, C. Dellago, and P. Geissler, Ann. Rev. Phys. Chem. **53**, 291 (2002).
 - [42] Y. S. Elmatad, R. L. Jack, J. P. Garrahan and D. Chandler, Proc. Nat. Acad. Sci. USA **107**, 12793 (2010).
 - [43] R. L. Jack, L. O. Hedges, J. P. Garrahan and D. Chandler, Phys. Rev. Lett. **107**, 275702 (2011).
 - [44] T. Speck, A. Malins and C. P. Royall, Phys. Rev. Lett. **109**, 195703 (2012)
 - [45] Y. S. Elmatad and R. L. Jack, J. Chem. Phys. **138**, 12A531 (2013).
 - [46] R. L. Jack, J. P. Garrahan and D. Chandler, J. Chem. Phys. **125**, 184509 (2006).
 - [47] S. Whitelam and J. P. Garrahan, J. Phys. Chem. B **108**, 6611 (2004)